Numerical Investigation of Time-Dependent Properties and Extinction of Strained Methane- and Propane-Air Flamelets

G. STAHL and J. WARNATZ

Institut für Technische Verbrennung der Universität Stuttgart, Pfaffenwaldring 12, Stuttgart, Germany

Laminar premixed strained flames are numerically modeled for time-dependent strain rates and pressure. The simulations include detailed chemistry in terms of a set of elementary reactions, as well as a multispecies transport model. The motivation to consider time dependence in modeling of strained flames is the consequence of the concept of strained laminar flamelets in unsteady turbulent combustion, such as occurs in internal combustion engines where the turbulent flow field and pressure are subject to large temporal variations.

Nonstationary conservation equations for strained flames have been derived including one-parameter (strain rate or tangential pressure gradient) and two-parameter (tangential pressure gradient and flow field divergence) formulations. These equations then have been used to study the following problems:

Extinction limits of methane–air flames at different equivalence ratios in the stationary case, to test the model and the input data used (e.g., different levels of methane oxidation chemistry).

Influence of temporally periodical change of the strain rate on the flame front behavior. Actually, a lean methane–air flame with sinusoidally varying strain rate is simulated numerically.

Influence of simultaneous application of strain and time-dependent pressure decrease, as occurs in the decompression phase in an Otto engine. A propane–air flame (starting at $P = 8$ bar) is used to elucidate pressure decrease at strain rate values typical in this environment.

Temporal behavior of a strained flame front to determine the characteristic extinction time. Lean and rich propane–air flames are considered during quenching under the influence of a constant strain rate.

The results are discussed and compared—as far as possible—with experimental and computational results given in the literature.

INTRODUCTION

Premixed laminar strained flames play an important role in turbulent combustion [1–3]. For flames of a thickness that is small compared with the turbulent length scale, turbulent combustion involves laminar flamelets that are wrinkled and torn by the turbulent flow field. The properties of the turbulent flame are calculated from an ensemble of laminar flamelets. This requires the calculation of a library of strained laminar flames containing scalar quantities as a function of equivalence ratio, pressure, temperature, and strain rate.

There have been several numerical studies of strained flames in counterflow configurations in recent years, both for a twin-flame configuration of two identically premixed flows of unburned gas impinging against each other (Fig. 1a) and a single-flame configuration with counterflowing unburned mixture and hot burned gases (Fig. 3a) [4–10]. A third configuration being investigated is the tubular flame, which was subject of a workshop in Leeds in April 1988 [34]. The specific interest of all these studies is to investigate the structure and the extinction limits of strained flames. Furthermore, experiments have been performed to study laminar flames in counterflow configurations with the same objectives [11–16]. The discrepancy between predicted and measured extinction strain rates has been discussed repeatedly [8,10].

In this article, extinction limits for strained methane–air flames have been calculated using two chemical reaction mechanisms. The first mechanism includes full C-3 chemistry, and the second involves C-1 species exclusively. The results are compared with calculations of Kee et al. [10] where a similar mechanism including C-1 and C-2 species is employed. Furthermore, the results are compared with an experiment by Law et al. for the twin flame configuration [16]. For

0010-2180/91/$3.50

this comparison, the traditional boundary layer approximation to calculate strained flames (in terms of the strain rate) has been utilized. This approach is equivalent to the one-parameter formulation in its steady-state limit outlined in this article (see Eq. 14 and Appendix A).

Recently it has been shown that diffusion flamelets follow variations of the strain rate in finite time, i.e., the flamelets do not respond quickly enough to changes of the strain rate [17]. Haworth et al. found this to be true in particular for low strain rates occurring far downstream in turbulent jet diffusion flames, thus requiring a modification of the flamelet model [17]. For premixed flamelets, Peters [2] suspected from stability investigations of strained premixed flames in random turbulent flow fields that a quasi-static description of the flamelets is inadequate.

Therefore, in this study the responses of premixed strained flames to changes of the turbulent flow field are investigated. Methane–air flamelets in a counterflow twin flame configuration are subject to strain (or equivalently to tangential pressure gradient) that is sinusoidally varied with time. The frequency covers the range from 20 to 500 Hz. In 1976, Saitoh and Otsuka [18] performed a counterflow experiment for ethylene flames in which they varied periodically the velocity at the burner nozzle. Keeping the amplitude of the velocity oscillation constant they observed oscillations of the luminous flame zone. The amplitude of the oscillations of the flame decreased with the frequency of the velocity oscillations. Changing the velocity at the burner nozzle in the experiment is equivalent to varying the strain rate in the numerical simulation.

Flamelet concepts of turbulent combustion require a library of strained laminar flamelets to model turbulent flames, for example, in an internal combustion engine. The flame in an internal combustion engine, however, suffers not only from strain but also from the cooling caused by the adiabatic pressure decrease due to expansion. Therefore, for constant strain rate, the heat release from the flame with decreasing pressure is investigated. This has been performed for the single flame counterflow configuration, which is more likely to be applied in models of turbulent combustion.

Several investigations of strained flames predict extinction of twin flames as either a Lewis-number effect or as a consequence of incomplete combustion and strain [11, 19–21]. It is observed experimentally that rich methane–air and lean propane–air twin flames are quenched before merging at the stagnation plane, whereas lean methane–air and rich propane–air twin flames extinguish at the stagnation plane [12, 13]. The extinction behavior of lean and rich propane–air flames is considered in this article and the results are compared with experiments.

ONE-PARAMETER FORMULATION

The geometries of the systems investigated are shown in Figs. 1a and 3a. Axisymmetric configurations have been regarded exclusively. The governing equations can be treated in terms of a single coordinate, if, according to Williams [22], the boundary layer approximations are applied to the reacting flow considered. This reduction to one single coordinate is very convenient for the numerical implementation, particularly if, as is done here, detailed chemistry is taken into account. The approach of Williams [22] is widely used for the stationary formulation of the problem [4–9], the governing equations of which are listed in Appendix A. The tangential pressure gradient divided by the coordinate r,$(1/r)(\partial P/\partial r)$, which is constant throughout the flow field, and the divergence of the flow field at the unburned edge of the boundary layer $(\partial v_r/\partial r)_{ub}$ are expressed in this formulation by a single parameter usually called strain rate a. For simplicity, $(1/r)(\partial P/\partial r)$ is called "tangential pressure gradient" in the following discussion.

TWO-PARAMETER FORMULATION FOR STATIONARY CASES

Kee et al. [10] extend this formulation to a two-parameter case. Starting (like Williams [22]) from the Navier–Stokes equations in two dimensions they succeed in formulating the problem in one space coordinate with two independent parameters, namely the tangential pressure gradient $(1/r)(\partial P/\partial r)$ and the divergence of the flow field at the burner nozzle $(\partial v_r/\partial r)_{nz}$, with $(1/r)(\partial P/\partial r)$ also being constant throughout the flowfield in this formulation. The latter approach is only applicable for the steady state and allows equally well the inclusion of an inhomogeneous flow field with zero divergence at the burner

nozzle. The equations are also given in Appendix A.

As mentioned by Kee et al. [10], the two-parameter approach is more general and therefore more appropriate to simulate experiments. The parameters provided by experimentalists could be the normal velocity component at the nozzle and one of the gradients $\partial v_z/\partial z$ or $\partial v_r/\partial r$ near the nozzle. In order to model an experimental counterflow configuration, the burner separation distance is equally essential. Providing these data by experiments and using the two-parameter approach for the numerical simulation, the quality of the chemical reaction mechanisms for strained flames, in particular those concerning extinction limits, could be studied. For applications in turbulent flames the one-parameter formulation of strained flames is convenient and probably a good approximation.

The specific intention of this work is to extend the applicability of the two-parameter approach to nonstationary problems, in particular to model time dependence of the strain rate and the pressure. From this, under conditions to be specified, a time-dependent formulation of the one-parameter problem with the tangential pressure gradient as parameter can be derived.

TWO-PARAMETER FORMULATION FOR NONSTATIONARY CASES

The formulation given by Kee et al. introduces a stream function that satisfies the stationary continuity equation identically this way excluding the treatment of unsteady problems (see Appendix A). However, the assumptions leading to the reduction of the formulation of the problem to one space coordinate do not exclude unsteady behavior. These assumptions are as follows:

1. the temperature and mass fractions of all species solely are a function of the coordinate normal to the flame z;
2. the normal velocity component v_z solely is a function of z;
3. the tangential velocity component v_r is proportional to the coordinate tangential to the flame r; the tangential velocity gradient $\partial v_r/\partial r = G$ therefore is solely dependent on z; and
4. the solutions are considered along the z axis, i.e., for $r = 0$, where the first derivative in radial direction of the density vanishes.

With ρ symbolizing the density, w_i the mass fraction of the chemical species i, T the temperature, and t the time, these conditions in time-dependent formulation read as

$$\frac{\partial T(z,r,t)}{\partial r} = \frac{\partial w_i(z,r,t)}{\partial r} \equiv 0,$$

$$\frac{\partial v_z(z,r,t)}{\partial r} \equiv 0,$$

$$\frac{\partial v_r(z,r,t)}{\partial r} = G(z,t) = \frac{v_r(z,r,t)}{r},$$

$$\left(\frac{\partial \rho(z,r,t)}{\partial r}\right)_{r=0} = 0.$$

Introducing these assumptions into the two-dimensional formulation of the continuity equation, Navier–Stokes equations, and the conservation equations for the enthalpy and mass fractions of the chemical species in cylindrical coordinates z an r, the following set of equations is obtained:

$$\frac{\partial \rho}{\partial t} + 2\rho G + \frac{\partial(\rho v_z)}{\partial z} = 0, \tag{1}$$

$$\frac{\partial G}{\partial t} + \frac{J}{\rho} + G^2 - \frac{1}{\rho}\frac{\partial}{\partial z}\left(\mu\frac{\partial G}{\partial z}\right) + v_z\frac{\partial G}{\partial z} = 0, \tag{2}$$

$$\frac{\partial v_z}{\partial t} + \frac{1}{\rho}\frac{\partial P}{\partial z} + \frac{4}{3\rho}\frac{\partial}{\partial z}(\mu G) - \frac{2\mu}{\rho}\frac{\partial G}{\partial z} - \frac{4}{3\rho}\frac{\partial}{\partial z}\left(\mu\frac{\partial v_z}{\partial z}\right) + v_z\frac{\partial v_z}{\partial z} = 0, \tag{3}$$

$$\frac{\partial T}{\partial t} - \frac{1}{\rho}\frac{\partial P}{\partial t} - \frac{1}{\rho c_p}\frac{\partial}{\partial z}\left(\lambda\frac{\partial T}{\partial z}\right) + \frac{1}{\rho c_p}\frac{\partial T}{\partial z}\sum_{i=1}^{n_s} c_{pi} j_{i,z} + \frac{1}{\rho c_p}\sum_{i=1}^{n_s}\dot{\omega}_i h_i M_i + v_z\frac{\partial T}{\partial z} = 0, \tag{4}$$

$$\frac{\partial w_i}{\partial t} + \frac{1}{\rho}\frac{\partial \cdot}{\partial z}(j_{i,z}) - \frac{\dot{\omega}_i M_i}{\rho} + v_z\frac{\partial w_i}{\partial z} = 0, \tag{5}$$

$$\rho - \frac{P\overline{M}}{RT} = 0, \tag{6}$$

with the tangential pressure gradient (P describes the pressure)

$$J = \frac{1}{r}\frac{\partial P}{\partial r} \tag{7}$$

and the diffusion fluxes

$$j_{i,z} = -\left(\rho D_i^F \frac{w_i}{x_i}\frac{\partial x_i}{\partial z} + \frac{D_i^T}{T}\frac{\partial T}{\partial z}\right).$$

According to Eqs. 2 and 3 we can write

$$J = \frac{1}{r}\frac{\partial P}{\partial r} = f(z,t), \qquad \frac{\partial P}{\partial z} = g(z,t),$$

i.e., both quantities are independent of r. With

$$\frac{\partial}{\partial z}\left(\frac{1}{r}\frac{\partial P}{\partial r}\right)_t = \frac{1}{r}\frac{\partial}{\partial r}\left(\frac{\partial P}{\partial z}\right)_t = 0, \tag{8}$$

one can conclude that $J = (1/r)(\partial P/\partial r)$ is a constant quantity throughout the flow field that varies with time. The pressure is introduced as an independent function of time.

PHYSICAL CHEMISTRY

The chemical production rates $\dot{\omega}_i$ are determined in the usual way (see e.g., Ref. 8) from a large number of elementary reactions listed in Appendix B, including the kinetic data from which the rate coefficient $k(T)$ for each reaction is calculated according to the Arrenhius type law

$$k(T) = AT^{\beta}\exp\left(\frac{-E}{RT}\right),$$

with A representing the preexponential factor, β the exponent of the temperature, and E the activation energy. The reactions and their rate coefficients result from a critical review of several hundred elementary reactions occurring in hydrocarbon combustion [23–26]. Thermochemical data are taken from the JANAF Tables [27]. As usual, c_p represents the specific heat capacity of the mixture at constant pressure, $c_{p,i}$ the specific heat capacity of the single chemical species i at constant pressure, M_i and h_i the molar mass and the specific enthalpy of the species i, $\overline{M}$ the mean molar mass of the mixture, and R the universal gas constant. The heat conductivity λ and the viscosity μ of the mixture and the coefficients of Fick's diffusion D_i^F and thermal diffusion D_i^T of species i are calculated according to Refs. 28 and 29.

INITIAL AND BOUNDARY CONDITIONS

The twin-flame counterflow configuration requires symmetrical boundary conditions at the stagnation plane as follows:

$$v_z = \frac{\partial G}{\partial z} = \frac{\partial T}{\partial z} = \frac{\partial w_i}{\partial z} = \frac{\partial \rho}{\partial z} = 0, \tag{9}$$

i.e, the velocity remains zero while the gradients of the other quantities (that may vary with time) vanish.

At the cold boundary (burner nozzle) the boundary conditions are

$$\begin{aligned} &v_z(t) = v_{z,nz}(t), \quad G(t) = G_{nz}(t), \\ &T(t) = T_{ub}(t), \quad w_i(t) = w_{i,ub}(t), \\ &\rho(t) = \rho_{ub}(t), \end{aligned} \tag{10}$$

i.e., all quantities at the burner nozzle can be introduced as a function of time. For the examples treated in this article the boundary values for the mass fractions $w_{i,ub}$ do not vary with time. For constant pressure the boundary conditions for the temperature as well as for the density are independent of the time. If the pressure varies with time, the boundary conditions for the temperature and the density are no longer constant. The temperature $T_{ub}(t)$ is determined from the actual pressure assuming adiabatic conditions according to the situation during the decompression phase of an Otto engine. The boundary value of the density $\rho_{ub}(t)$ is determined from the actual pressure and the temperature $T_{ub}(t)$ by the ideal gas equation of state.

Starting the time integration, steady-state solutions are employed as initial conditions.

$G_{nz}(t)$ and $v_{z,nz}(t)$ are two parameters to be chosen independently. The tangential pressure gradient $J(t)$ then is determined. It is also possible to introduce $J(t)$ and $G_{nz}(t)$ and calculate $v_{z,nz}(t)$ as a part of the solution. Generally, two parameters of the triple set (J, $v_{z,nz}$, G_{nz}) have to be known. The respective third can then be determined. This results from the coupling of Eqs. 1 and 2.

It easily can be shown that in the case of steady

solutions the two-parameter equations (Eqs. 1–7) presented above are identical to those proposed by Kee et al. [10] (see Appendix A).

REDUCTION TO A ONE-PARAMETER FORMULATION FOR NONSTATIONARY CASES

In this investigation, a one-parameter formulation of the nonstationary equations (see below) has been adopted, because there is no information available about a second parameter.

From the equations presented above, it can be seen that the two-parameter problem is reduced to a one-parameter problem if the spatial derivatives of $G(z, t)$ at the burner nozzle remain zero:

$$\left(\frac{\partial G}{\partial z}\right)_{nz}(t) = \left(\frac{\partial^2 G}{\partial z^2}\right)_{nz}(t) \equiv 0.$$

With Eq. 2 it then follows

$$J(t) = -\rho_{ub}(t)\left(G_{nz}^2(t) + \left(\frac{\partial G(t)}{\partial t}\right)_{nz}\right), \tag{11}$$

i.e., $J(t)$ and $G_{nz}(t)$ now are related to one another. In the one-parameter restriction, therefore, only one parameter of the triple set $(J, v_{z,nz}, G_{nz})$ has to be prescribed. Furthermore, it is not possible to describe strained flames with zero divergence of the flow field to the burner nozzle, because, according to Eq. 11, $J(t)$ vanishes as well for $G_{nz}(t) \equiv 0$.

The boundary conditions for the derivatives of G are met if the density is spatially constant and if the normal velocity decreases (increases) linearly with z (see Eq. 1). This corresponds to potential flow at the edges of the configuration of Fig. 1a.

In this one-parameter formulation for constant ρ_{ub} the tangential pressure gradient $J(t)$ can be introduced as a function of time. The value of $G_{nz}(t)$ results implicitly from the boundary conditions $(\partial G/\partial z)_{nz}(t) = (\partial^2 G/\partial z^2)_{nz}(t) \equiv 0$. An alternate possibility is to calculate $G_{nz}(t)$ according to Eq. 11 from $J(t)$ and the initial value $G_{nz}(t = 0)$. In the case of the introduction of $G_{nz}(t)$ as a function of time, $J(t)$ is easily determined from Eq. 11.

For temporally varying pressure the density at the burner nozzle $\rho_{ub}(t)$ is a function of time. Either $J(t)$ or $G_{nz}(t)$ can be kept constant in this case. It is also possible to have all three quantities $J(t)$, $G_{nz}(t)$, and $\rho_{ub}(t)$ time dependent. Thereby, $\rho_{ub}(t)$ describes the history of the pressure and $J(t)$ or $G_{nz}(t)$ the history of the flowfield to be arbitrarily varied with time.

Boundary conditions for the one-parameter formulation are explicitly given below. For both the twin and single-flame configuration, boundary conditions on the unburned side are

$$v_z(t) = v_{z,nz}(t) \quad \text{or} \quad G(t) = G_{nz}(t)$$

$$\text{or} \quad J = J(t),$$

$$T(t) = T_{ub}(t), \quad w_i(t) = w_{i,ub}(t),$$

$$\rho(t) = \rho_{ub}(t).$$

The boundary conditions at the stagnation plane for the twin flames (Fig. 1a) in the one-parameter description are identical to those in the two-parameter formulation (see Eq. 9). For the single-flame configuration (Fig. 3a) the following boundary conditions apply on the burned side:

$$v_z(t) = v_{z,b}(t), \quad G(t) = G_b(t),$$

$$T(t) = T_b(t), \quad w_i(t) = w_{i,b}(t),$$

$$\rho(t) = \rho_b(t).$$

The one-parameter description requires the assumption of potential flow for the burned gases as well

$$\left(\frac{\partial G}{\partial z}\right)_b(t) = \left(\frac{\partial^2 G}{\partial z^2}\right)_b(t) \equiv 0. \tag{12}$$

The divergence of the flow field on the burned side $G_b(t)$ and $J(t)$ are then correlated according to Eq. 2:

$$J(t) = -\rho_b(t)\left(G_b{}^2(t) + \left(\frac{\partial G(t)}{\partial t}\right)_b\right). \tag{13}$$

$J(t)$ is already known from the conditions on the unburned side, for it is constant throughout the flowfield, and $G_b(t = 0)$ is determined from the steady-state solution, which in turn can be calcu-

lated from $G_{nz}(t = 0)$:

$$G_b(t = 0) = G_{nz}(t = 0)\sqrt{\frac{\rho_{ub}(t = 0)}{\rho_b(t = 0)}} .$$

This follows for steady conditions from the constant tangential pressure gradient J (Eqs. 11 and 13). However, $G_b(t)$ is more easily adjusted by the boundary conditions of Eq. 12. The value for the velocity on the burned side $v_{z,b}(t)$ must be specified. The time-dependent boundary conditions for the temperature and the density are determined as described above for the two-parameter equations. The mole fractions on the hot side in the single-flame configuration generally are not known. In this work they are set to the equilibrium values at the corresponding temperature $T_b(t)$.

Finally, it should be mentioned that the quantities $J = (1/r)(\partial P/\partial r)$ and the strain rate a of the traditional formulation are correlated in a simple way, if one assumes potential flow at the cold edge and considers steady state:

$$J = -\rho_{ub}a^2. \qquad (14)$$

This follows from the definition of $(1/r)(\partial P/\partial r)$ in the traditional formulation (steady potential flow) (see Appendix A).

Solution of the Conservation Equations

The system of partial differential and algebraic Eqs. 1, 2, and 4–6 can be solved numerically. Spatial discretization using finite differences on a statically adapted grid point system leads to a system of ordinary differential equations in time and algebraic equations. In addition to the ideal gas equation of state, the continuity equation (after spatial discretization) is treated as an algebraic equation for v_z. The time derivative of the density is determined from the residuals of the temperature and the mass fractions and the prescribed time dependence of the pressure. For the adaption of the grid point system see Ref. 30. Due to the stiffness introduced by the chemical kinetics, an implicit method with internal order and stepsize control must be used for the solution of the system of ordinary differential and algebraic equations. As backward-differencing methods suffer from the low efficiency in the initialization phase (necessary after a static grid point adaption), an extrapolation method developed by Deuflhard and coworkers is used [31–33]. Efficiency is improved by making use of the block tridiagonal structure of the Jacobian both in its numerical evaluation and in the solution of the linear equation systems resulting from the time discretion.

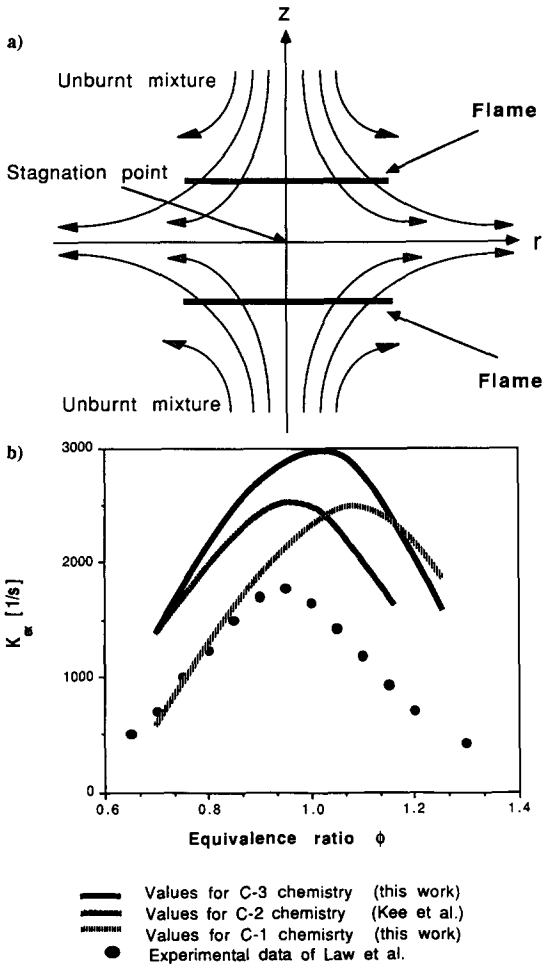

Fig. 1. (a) Axisymmetric twin flame configuration for strained flames. (b) Extinction limits of strained premixed methane–air flames as a function of equivalence ratio; comparison of calculated results for three different mechanisms of two different groups and experiment; $K = 2a$ for axisymmetric configuration.

RESULTS AND DISCUSSION

Stationary Flames

Figure 1b shows a detailed study of the influence of the chemical reaction mechanism adopted on calculated extinction limits for strained methane–

air flames. Also the experimental data of Law et al. [16] are marked. The numerical results originate from Kee et al. [10] and this work. All of them are obtained using the traditional boundary layer approximation for strained flames (see Appendix A). The results apply to the twin-flame configuration depicted schematically in Fig. 1a. With regard to lean conditions first the mechanism consisting of C-1 species alone predicts extinction strain rates that are even less than the experimental values. The position of the maximum, however, is not met at all by the C-1 mechanism, with incorrect results on the rich side. The results for the mechanisms with up to C-2 and C-3 species are in good agreement on the lean side, but differ significantly for stoichiometric to rich conditions, indicating that C-3 species play an increasingly important role with increasing methane concentration. It should be mentioned that the results for the C-3 mechanism and the C-2 mechanism are from two different research groups. The coincidence of the values on the lean side indicates that both mechanisms are very similar concerning C-1 and C-2 species. The results for both mechanisms using species with more than one C atom lie well above the experimental values. This might also be due to errors in the modeling of the chemistry, especially on the rich side, but it seems likely that the one-parameter description of the problem is partly responsible for the discrepancy between simulation and experiment. As already mentioned, for a more realistic one-dimensional modeling of strained flames experiments, more information about the flow field is required.

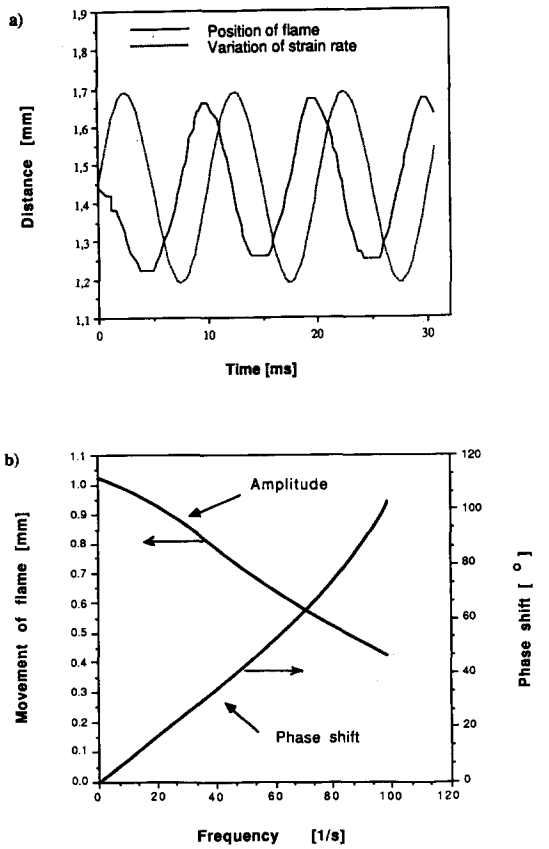

Fig. 2. (a) Oscillation of flame for frequency of 100 oscillations per second of strain rate (tangential pressure gradient J); lean methane–air flame; twin-flame configuration. (b) Behavior of amplitude and phase shift of flame oscillation with increasing frequency of the oscillation of the strain rate (tangential pressure gradient J); lean methane–air flame.

Nonstationary Flames

Time-Dependent Strain Rate. We now turn away from strained flames in the steady state and consider premixed flames subjected to time-dependent strain rates. This is motivated by experimental results [18] and by considerations of time-dependent strain rates in turbulent diffusion flames [17] as well as theoretical studies on the stability of premixed flames [2]. In this study we have varied the tangential pressure gradient $J(t)$. This quantity is equivalent to the strain rate in the traditional formulation (see Eq. 14). Changing the velocity at the nozzle $v_{z,nz}$ (as in the experiment [18]) is equivalent to changing the tangential pressure gradient $J(t)$, as has been shown for the one-parameter formulation. According to the experiment we have chosen sinusoidal variation with time of the quantity $J(t)$ in a twin-flame configuration. The amplitude of the variation of $J(t)$ is 50% of its value in steady state. For a frequency of 100 oscillations per second, Fig. 2a shows the variation of $J(t)$ (shifted profile in arbitrary units) and the typical response of the flame. The position of the flame (defined as the distance of the location of the maximum fuel consumption from the stagnation point) is varied approximately sinusoidally with time. A well-defined phase shift between $J(t)$ and the response of the flame can be observed after the first period. The "amplitude" of the oscillation of the flame, defined as the difference

between the minimum and the maximum value of the flame position, is nearly constant. The deviation of the flame movement from the ideal sinusoidal shape results from the nonlinear relationship between flame position and strain rate [$J(t)$], especially for small distances between the flame center and the stagnation plane [8]. We have chosen the steady-state solution at a corresponding strain rate of about 150 s^{-1} as initial conditions for a lean methane–air flame ($\Phi = 0.7$) with a chemical reaction mechanism consisting of C-1 species only.

The dependence of the phase shift and the "amplitude" on the frequency is shown in Fig. 2b. It can be seen that for low frequencies the flame follows nearly instantaneously the variation of the strain rate. However, for 80 oscillations per second the amplitude has dropped already by 50% while the phase shift has increased to 75°. For a frequency of 500 s^{-1} (not shown) the flame is no longer reacting to the variations of the strain rate. It remains in the steady-state position according to the strain rate of about 150 s^{-1}. These results reflect qualitatively the experimental results of Saitoh and Otsuka for ethylene flames [18].

Typical time scales of the chemical reaction in laminar hydrocarbon flames are of the order of a millisecond. We have shown that remarkable deviations occur in the response of the flame to variations of the flow field at time scales for such variations that are 10–20 times larger than the time scale of the chemistry. This relation of the time scales corresponds to large Damköhler numbers. Within the range of the applicability of the flamelet model, therefore, premixed flamelets do not seem to respond instantaneously to changes of the turbulent flow field.

Time-Dependent Pressure. A lean propane–air flame ($\Phi = 0.8$) at a constant tangential pressure gradient J of 10^7 N/m^4 was subjected to a linear pressure decrease of 2 bar/ms. For the initial conditions a steady burning single flame at 8 bar was chosen, with the hot burned gases in thermal equilibrium at the adiabatic flame temperature. The initial value of the temperature of the unburned gases is set to 300 K. In this way the influence of the adiabatic pressure decrease on the strained flamelets in an internal combustion engine during the expansion phase after the ignition can be estimated. In Fig. 3a the single-

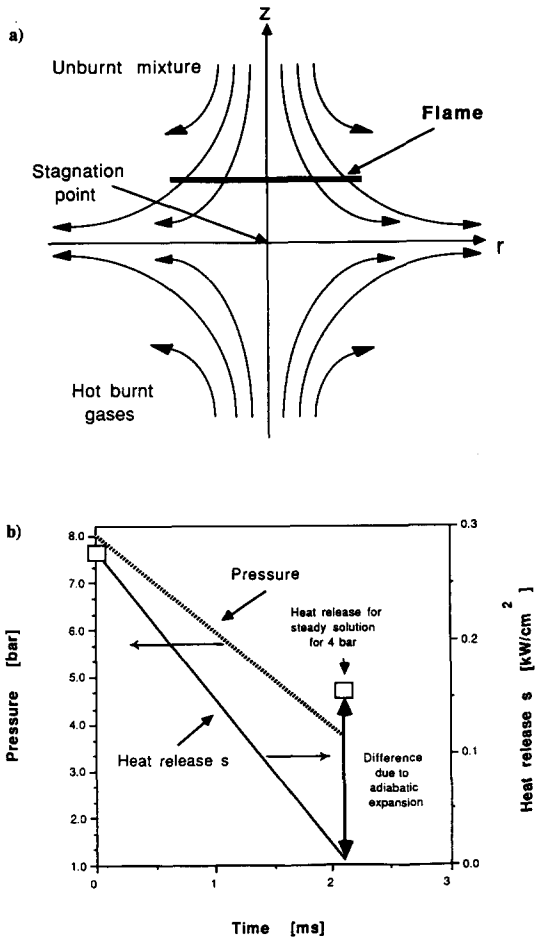

Fig. 3. (a) Axisymmetric single-flame configuration for strained flames. (b) Heat release per unit flame area s during nonstationary pressure decrease for a lean propane–air flame; contribution of the adiabatic heat loss; single-flame configuration.

flame configuration is shown. As a measure of the burning rate of strained flamelets, the heat release per unit flame area s has been used in this work:

$$s = \int_{-\infty}^{\infty} \sum_{i=1}^{n_s} (\dot{\omega}_i M_i h_i)\, dz.$$

The meaning of the symbols is explained in the section on Physical Chemistry. The square symbols in Fig. 3b represent the heat release per unit flame area for steady flames for pressures of 8 and 4 bar. As indicated, the solid line describes the heat release, whereas the broken one represents the pressure decrease with time. For the conditions specified the adiabatic expansion has a

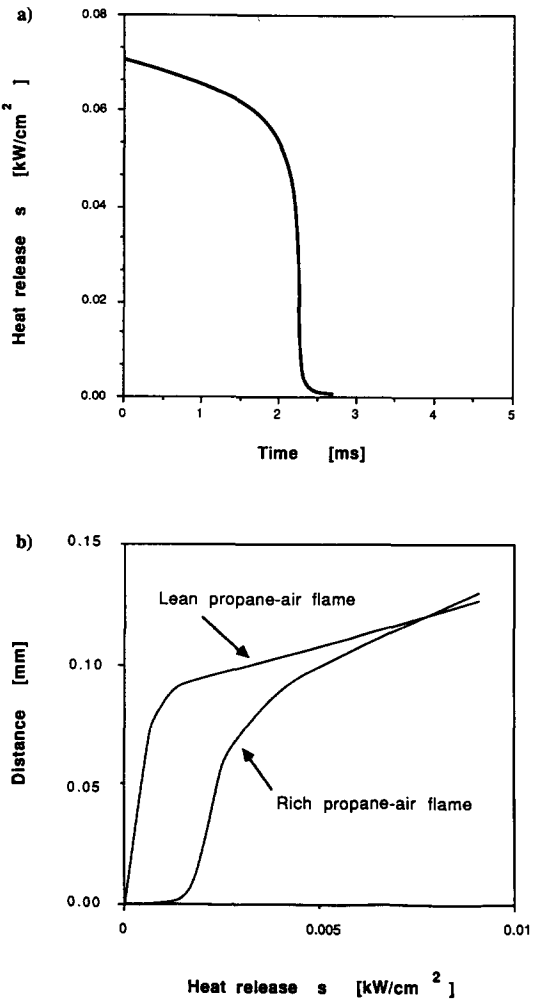

Fig. 4. (a) Typical profile of heat release per unit flame area s during extinction of a strained hydrocarbon flame; twin-flame configuration. (b) Distance of flame center from stagnation point as a function of heat release per unit flame area s during extinction; comparison of lean and rich propane-air flames, twin-flame configuration.

great influence (arrow) on the heat release and therefore burning rate of the flame. Although these conditions are unlikely to be valid in real engines, this example shows that in addition to possible extinction by high strain rates laminar flames also can extinguish due to cooling in an adiabatic expansion.

Extinction Behavior. Finally, in Fig. 4a the extinction behavior of strained twin flames is monitored. The heat release per unit flame area is plotted against time. For the initial condition a steadily burning flame close to extinction has been selected. The tangential pressure gradient $J(t)$ is set instantaneously to a value beyond extinction. For lean and rich methane- and propane-air flames the same characteristics are observed: the heat release slowly approaches a value, from which it drops steeply to zero within half a millisecond. The flame position (location of maximum fuel consumption) during extinction is compared between a lean propane-air flame ($\Phi = 0.8$) and a rich propane-air flame ($\Phi = 1.72$) in Fig. 4b. The lean flame reaches the stagnation plane virtually quenched (the heat release has vanished), whereas the rich flame arrives at the stagnation plane while there is still some heat release. This result is in qualitative agreement with the experimental findings of Tsuji and Yamaoka [12] and Sato [13]: lean propane-air flames extinguish before they have merged at the stagnation plane, but rich propane-air flames are observed to quench very close to each other.

APPENDIX A

Boundary Layer Approximation for Strained Flames (in terms of the strain rate a for steady axisymmetric flows)

$$\frac{1}{r}\frac{\partial P}{\partial r} = -\rho_{ub}a^2,$$

$$\frac{\partial v_r}{\partial r} = af' = \frac{v_r}{r},$$

$$2\rho a f' + \frac{\partial(\rho v_z)}{\partial z} = 0,$$

$$a\left(f'^2 - \frac{\rho_{ub}}{\rho}\right) + v_z\frac{\partial f'}{\partial z} - \frac{1}{\rho}\frac{\partial}{\partial z}\left(\mu\frac{\partial f'}{\partial z}\right) = 0,$$

$$-\frac{1}{\rho c_p}\frac{\partial}{\partial z}\left(\lambda\frac{\partial T}{\partial z}\right) + \frac{1}{\rho c_p}\frac{\partial T}{\partial z}\sum_{i=1}^{n_s} c_{pi}j_{i,z} + \frac{1}{\rho c_p}\sum_{i=1}^{n_s}\dot{\omega}_i h_i M_i + v_z\frac{\partial T}{\partial z} = 0,$$

$$\frac{1}{\rho}\frac{\partial}{\partial z}(j_{i,z}) - \frac{\dot{\omega}_i M_i}{\rho} + v_z\frac{\partial w_i}{\partial z} = 0,$$

$$\rho - \frac{P\overline{M}}{RT} = 0,$$

$$j_{i,z} = -\left(\rho D_i^D\frac{w_i}{x_i}\frac{\partial x_i}{\partial z} + \frac{D_i^T}{T}\frac{\partial T}{\partial z}\right).$$

The boundary conditions for twin flames (Fig. 1a) at the stagnation plane are

$$v_z = \frac{\partial f'}{\partial z} = \frac{\partial T}{\partial z} = \frac{\partial w_i}{\partial z} = 0.$$

At the cold edge, the boundary conditions are

$$f' = 1, \quad T = T_{ub}, \quad w_i = w_{i,ub}$$

a is introduced as an input parameter

Boundary conditions for the single-flame configuration (Fig. 3a) at the hot edge are

$$v_z = v_{z,b}, \quad f' = \sqrt{\frac{\rho_{ub}}{\rho_b}},$$

$$T = T_b, \quad w_i = w_{i,b}.$$

At the cold edge the boundary conditions are the same as for the twin-flame configuration (see above).

Equations Proposed by Kee et al. [10]

$$\rho v_z = -2F(z),$$

$$\rho v_r = r\frac{dF(z)}{dz},$$

$$\frac{\partial F}{\partial z} = \rho G,$$

$$\frac{J}{\rho} + G^2 - \frac{1}{\rho}\frac{\partial}{\partial z}\left(\mu\frac{\partial G}{\partial z}\right) - \frac{2F}{\rho}\frac{\partial G}{\partial z} = 0,$$

$$\frac{\partial P}{\partial z} + \frac{4}{3}\frac{\partial}{\partial z}(\mu G) - 2\mu\frac{\partial G}{\partial z}$$

$$+\frac{8}{3}\frac{\partial}{\partial z}\left(\mu\frac{\partial}{\partial z}\left(\frac{F}{\rho}\right)\right)$$

$$+4F\frac{\partial}{\partial z}\left(\frac{F}{\rho}\right) = 0,$$

$$\frac{1}{\rho c_p}\frac{\partial T}{\partial z}\sum_{i=1}^{n_s} c_{pi} j_{i,z} - \frac{1}{\rho c_p}\frac{\partial}{\partial z}\left(\lambda\frac{\partial T}{\partial z}\right)$$

$$+\frac{1}{\rho c_p}\sum_{i=1}^{n_s}\dot{\omega}_i h_i M_i - \frac{2F}{\rho}\frac{\partial T}{\partial z} = 0,$$

$$\frac{1}{\rho}\frac{\partial}{\partial z}(j_{i,z}) - \frac{\dot{\omega}_i M_i}{\rho} - \frac{2F}{\rho}\frac{\partial w_i}{\partial z} = 0,$$

$$\rho - \frac{P\bar{M}}{RT} = 0,$$

$$J = \frac{1}{r}\frac{\partial P}{\partial r},$$

$$j_{i,z} = -\left(\rho D_i^D \frac{w_i}{x_i}\frac{\partial x_i}{\partial z} + \frac{D_i^T}{T}\frac{\partial T}{\partial z}\right).$$

Boundary conditions for twin flames at the stagnation plane are

$$\frac{\partial T}{\partial z} = \frac{\partial w_i}{\partial z} = \frac{\partial G}{\partial z} = 0, \qquad F = 0$$

and at the cold edge (burner nozzle) are

$$T = T_{ub}, \quad w_i = w_{i,ub},$$

$$G = G_{nz}, \quad F = -\frac{\rho v_{z,nz}}{2}$$

J is calculated as an eigenvalue.

APPENDIX B [23-26]

CHEMICAL REACTION MECHANISM

	Mechanism						A (cm/mol/s)	Exp of T	E (kJ/mol)
				1. H_2-O_2 Mechanism					
1	O_2	+H		→ OH	+O		2.20E + 14	0.00	70.30
2	OH	+0		→ O_2	+H		1.72E + 13	0.00	3.52
3	H_2	+0		→ OH	+H		5.06E + 04	2.67	26.30
4	OH	+H		→ H_2	+O		2.22E + 04	2.67	18.29
5	H_2	+OH		→ H_2O	+H		1.00E + 08	1.60	13.80
6	H_2O	+H		→ H_2	+OH		4.31E + 08	1.60	76.46
7	OH	+OH		→ H_2O	+O		1.50E + 09	1.14	0.42
8	H_2O	+O		→ OH	+OH		1.47E + 10	1.14	71.09
9	H	+H	+M*	→ H_2	+M*		1.80E + 18	−1.00	0.00
10	H_2	+M*		→ H	+H	+M*	7.26E + 18	−1.00	436.82
11	H	+OH	+M*	→ H_2O	+M*		2.20E + 22	−2.00	0.00

CHEMICAL REACTION MECHANISM (*Continued*)

	Mechanism						*A* (cm/mol/s)	Exp of T	*E* (kJ/mol)
12	H_2O	$+M^*$		$\rightarrow H$	$+OH$	$+M^*$	3.83E + 23	−2.00	499.48
13	O	$+O$	$+M^*$	$\rightarrow O_2$	$+M^*$		2.90E + 17	−1.00	0.00
14	O_2	$+M^*$		$\rightarrow O$	$+O$	$+M^*$	6.55E + 18	−1.00	495.58
15	H	$+O_2$	$+M^*$	$\rightarrow HO_2$	$+M^*$		2.30E + 18	−0.80	0.00
16	HO_2	$+M^*$		$\rightarrow H$	$+O2$	$+M^*$	3.19E + 18	−0.80	195.39
17	HO_2	$+H$		$\rightarrow OH$	$+OH$		1.50E + 14	0.00	4.20
18	OH	$+OH$		$\rightarrow HO_2$	$+H$		1.50E + 13	0.00	170.84
19	HO_2	$+H$		$\rightarrow H_2$	$+O_2$		2.50E + 13	0.00	2.90
20	H_2	$+O_2$		$\rightarrow HO_2$	$+H$		7.27E + 13	0.00	244.33
21	HO_2	$+H$		$\rightarrow H_2O$	$+O$		3.00E + 13	0.00	7.20
22	H_2O	$+O$		$\rightarrow HO_2$	$+H$		2.95E + 13	0.00	244.51
23	HO_2	$+O$		$\rightarrow OH$	$+O_2$		1.80E + 13	0.00	−1.70
24	OH	$+O_2$		$\rightarrow HO_2$	$+O$		2.30E + 13	0.00	231.71
25	HO_2	$+OH$		$\rightarrow H_2O$	$+O_2$		6.00E + 13	0.00	0.00
26	H_2O	$+O_2$		$\rightarrow HO_2$	$+OH$		7.52E + 14	0.00	304.09
27	HO_2	$+HO_2$		$\rightarrow H_2O_2$	$+O_2$		2.50E + 11	0.00	−5.20
28	OH	$+OH$	$+M^*$	$\rightarrow H_2O_2$	$+M^*$		3.25E + 22	−2.00	0.00
29	H_2O_2	$+M^*$		$\rightarrow OH$	$+OH$	$+M^*$	1.69E + 24	−2.00	202.29
30	H_2O_2	$+H$		$\rightarrow H_2$	$+HO_2$		1.70E + 12	0.00	15.70
31	H_2	$+HO_2$		$\rightarrow H_2O_2$	$+H$		1.32E + 12	0.00	83.59
32	H_2O_2	$+H$		$\rightarrow H_2O$	$+OH$		1.00E + 13	0.00	15.00
33	H_2O	$+OH$		$\rightarrow H_2O_2$	$+H$		3.34E + 12	0.00	312.19
34	H_2O_2	$+O$		$\rightarrow OH$	$+HO_2$		2.80E + 13	0.00	26.80
35	OH	$+HO_2$		$\rightarrow H_2O_2$	$+O$		9.51E + 12	0.00	86.68
36	H_2O_2	$+OH$		$\rightarrow H_2O$	$+HO_2$		5.40E + 12	0.00	4.20
37	H_2O	$+HO_2$		$\rightarrow H_2O_2$	$+OH$		1.80E + 13	0.00	134.75
	2. $CO-CO_2$ Mechanism								
38	CO	$+OH$		$\rightarrow CO_2$	$+H$		4.40E + 06	1.50	−3.10
39	CO_2	$+H$		$\rightarrow CO$	$+OH$		4.97E + 08	1.50	89.74
40	CO	$+HO_2$		$\rightarrow CO_2$	$+OH$		1.50E + 14	0.00	98.70
41	CO_2	$+OH$		$\rightarrow CO$	$+HO_2$		1.70E + 15	0.00	358.18
42	CO	$+O$	$+M^*$	$\rightarrow CO_2$	$+M^*$		7.10E + 13	0.00	−19.00
43	CO_2	$+M^*$		$\rightarrow CO$	$+O$	$+M^*$	1.42E + 16	0.00	502.65
44	CO	$+O_2$		$\rightarrow CO_2$	$+O$		2.50E + 12	0.00	200.00
45	CO_2	$+O$		$\rightarrow CO$	$+O_2$		2.21E + 13	0.00	226.07
	3. C-1 Mechanism								
46	CH	$+O$		$\rightarrow CO$	$+H$		4.00E + 13	0.00	0.00
47	CO	$+H$		$\rightarrow CH$	$+O$		1.94E + 15	0.00	736.25
48	CH	$+O_2$		$\rightarrow CHO$	$+O$		3.00E + 13	0.00	0.00
49	CHO	$+O$		$\rightarrow CH$	$+O_2$		4.00E + 13	0.00	301.00
50	CH	$+CO_2$		$\rightarrow CHO$	$+CO$		3.40E + 12	0.00	2.90
51	CHO	$+H$		$\rightarrow CO$	$+H_2$		2.00E + 14	0.00	0.00
52	CO	$+H_2$		$\rightarrow CHO$	$+H$		1.30E + 15	0.00	376.50
53	CHO	$+O$		$\rightarrow CO$	$+OH$		3.00E + 13	0.00	0.00
54	CO	$+OH$		$\rightarrow CHO$	$+O$		8.56E + 13	0.00	368.48
55	CHO	$+O$		$\rightarrow CO_2$	$+H$		3.00E + 13	0.00	0.00
56	CO_2	$+H$		$\rightarrow CHO$	$+O$		9.66E + 15	0.00	461.33
57	CHO	$+OH$		$\rightarrow CO$	$+H_2O$		1.00E + 14	0.00	0.00
58	CO	$+H_2O$		$\rightarrow CHO$	$+OH$		2.80E + 15	0.00	439.16
59	CHO	$+O_2$		$\rightarrow CO$	$+HO_2$		3.00E + 12	0.00	0.00
60	CO	$+HO_2$		$\rightarrow CHO$	$+O_2$		6.70E + 12	0.00	135.07
61	CHO	$+M^*$		$\rightarrow CO$	$+H$	$+M^*$	7.10E + 14	0.00	70.30
62	CO	$+H$	$+M^*$	$\rightarrow CHO$	$+M^*$		1.14E + 15	0.00	9.98
63	CH_2	$+H$		$\rightarrow CH$	$+H_2$		8.40E + 09	1.50	1.40
64	CH	$+H_2$		$\rightarrow CH_2$	$+H$		5.83E + 09	1.50	13.96
65	CH_2	$+O$		$\rightarrow CO$	$+H$	$+H$	8.00E + 13	0.00	0.00
66	CH_2	$+O_2$		$\rightarrow CO$	$+OH$	$+H$	6.50E + 12	0.00	6.30

CHEMICAL REACTION MECHANISM (*Continued*)

	Mechanism						*A* (cm/mol/s)	Exp of T	*E* (kJ/mol)
67	CH_2	$+O_2$		$\rightarrow CO_2$	$+H$	$+H$	6.50E + 12	0.00	6.30
68	CH_2O	$+H$		$\rightarrow CHO$	$+H_2$		2.50E + 13	0.00	16.70
69	CHO	$+H_2$		$\rightarrow CH_2O$	$+H$		1.99E + 12	0.00	78.01
70	CH_2O	$+O$		$\rightarrow CHO$	$+OH$		3.50E + 13	0.00	14.60
71	CHO	$+OH$		$\rightarrow CH_2O$	$+O$		1.22E + 12	0.00	67.90
72	CH_2O	$+OH$		$\rightarrow CHO$	$+H_2O$		3.00E + 13	0.00	5.00
73	CHO	$+H_2O$		$\rightarrow CH_2O$	$+OH$		1.03E + 13	0.00	128.97
74	CH_2O	$+HO_2$		$\rightarrow CHO$	$+H_2O_2$		1.00E + 12	0.00	33.50
75	CHO	$+H_2O_2$		$\rightarrow CH_2O$	$+HO_2$		1.03E + 11	0.00	26.92
76	CH_2O	$+CH_3$		$\rightarrow CHO$	$+CH_4$		1.00E + 11	0.00	25.50
77	CHO	$+CH_4$		$\rightarrow CH_2O$	$+CH_3$		2.10E + 11	0.00	90.13
78	CH_2O	$+M^*$		$\rightarrow CHO$	$+H$	$+M^*$	1.40E + 17	0.00	320.00
79	CHO	$+H$	$+M^*$	$\rightarrow CH_2O$	$+M^*$		2.76E + 15	0.00	−55.51
80	CH_3	$+H$		$\rightarrow CH_2$	$+H_2$		1.80E + 14	0.00	63.00
81	CH_2	$+H_2$		$\rightarrow CH_3$	$+H$		3.63E + 13	0.00	44.53
82	CH_3	$+H$		$\rightarrow CH_4$			1.90E + 36	−7.00	38.00
83	CH_4			$\rightarrow CH_3$	$+H$		2.02E + 38	−7.00	478.13
84	CH_3	$+O$		$\rightarrow CH_2O$	$+H$		7.00E + 13	0.00	0.00
85	CH_2O	$+H$		$\rightarrow CH_3$	$+O$		9.23E + 14	0.00	292.53
86	CH_3	$+CH_3$		$\rightarrow C_2H_6$			1.70E + 53	−12.00	81.20
87	C_2H_6			$\rightarrow CH_3$	$+CH_3$		2.34E + 56	−12.00	446.61
88	CH_3	$+M$		$\rightarrow CH_2$	$+H$	$+M$	1.00E + 16	0.00	380.00
89	CH_2	$+H$	$+M$	$\rightarrow CH_3$	$+M$		5.01E + 14	0.00	−75.29
90	CH_3	$+CH_3$		$\rightarrow C_2H_4$	$+H_2$		1.00E + 16	0.00	134.00
91	CH_3	$+CH_2$		$\rightarrow C_2H_4$	$+H$		4.00E + 13	0.00	0.00
92	CH_4	$+H$		$\rightarrow H_2$	$+CH_3$		2.20E + 04	3.00	36.60
93	H_2	$+CH_3$		$\rightarrow CH_4$	$+H$		8.33E + 02	3.00	33.28
94	CH_4	$+O$		$\rightarrow OH$	$+CH_3$		1.20E + 07	2.10	31.90
95	OH	$+CH_3$		$\rightarrow CH_4$	$+O$		1.99E + 05	2.10	20.57
96	CH_4	$+OH$		$\rightarrow H_2O$	$+CH_3$		1.60E + 06	2.10	10.30
97	H_2O	$+CH_3$		$\rightarrow CH_4$	$+OH$		2.61E + 05	2.10	69.64
98	CH_4	$+HO_2$		$\rightarrow H_2O_2$	$+CH_3$		4.00E + 12	0.00	81.20
99	H_2O_2	$+CH_3$		$\rightarrow CH_4$	$+HO_2$		1.96E + 11	0.00	9.99
100	CH_4	$+CH_2$		$\rightarrow CH_3$	$+CH_3$		1.30E + 13	0.00	39.90
101	CH_3	$+CH_3$		$\rightarrow CH_4$	$+CH_2$		2.44E + 12	0.00	55.06
102	CH_4	$+CH$		$\rightarrow C_2H_4$	$+H$		3.00E + 13	0.00	−1.70
103	C_2H_4	$+H$		$\rightarrow CH_4$	$+CH$		4.45E + 14	0.00	237.19
			4. C-2 Mechanism						
104	C_2H	$+O$		$\rightarrow CO$	$+CH$		1.00E + 13	0.00	0.00
105	CO	$+CH$		$\rightarrow C_2H$	$+O$		1.32E + 13	0.00	309.38
106	C_2H	$+H_2$		$\rightarrow C_2H_2$	$+H$		1.10E + 13	0.00	12.00
107	C_2H_2	$+H$		$\rightarrow C_2H$	$+H_2$		1.08E + 14	0.00	96.59
108	C_2H	$+O_2$		$\rightarrow C_2HO$	$+O$		5.00E + 13	0.00	6.30
109	C_2HO	$+O$		$\rightarrow C_2H$	$+O_2$		2.14E + 14	0.00	274.56
110	C_2HO	$+H$		$\rightarrow CH_2$	$+CO$		3.00E + 13	0.00	0.00
111	CH_2	$+CO$		$\rightarrow C_2HO$	$+H$		2.38E + 12	0.00	−30.20
112	C_2HO	$+O$		$\rightarrow CO$	$+CO$	$+H$	1.00E + 14	0.00	0.00
113	C_2H_2	$+O$		$\rightarrow CH_2$	$+CO$		4.10E + 08	1.50	7.10
114	CH_2	$+CO$		$\rightarrow C_2H_2$	$+O$		7.93E + 07	1.50	219.33
115	C_2H_2	$+O$		$\rightarrow C_2HO$	$+H$		4.30E + 14	0.00	50.70
116	C_2HO	$+H$		$\rightarrow C_2H_2$	$+O$		1.05E + 15	0.00	293.13
117	C_2H_2	$+OH$		$\rightarrow H_2O$	$+C_2H$		1.00E + 13	0.00	29.30
118	H_2O	$+C_2H$		$\rightarrow C_2H_2$	$+OH$		4.39E + 12	0.00	7.37
119	C_2H_2	$+M$		$\rightarrow C_2H$	$+H$	$+M$	3.60E + 16	0.00	446.00
120	C_2H	$+H$	$+M$	$\rightarrow C_2H_2$	$+M$		9.08E + 14	0.00	−75.40
121	CH_2CO	$+H$		$\rightarrow CH_3$	$+CO$		7.00E + 12	0.00	12.60

CHEMICAL REACTION MECHANISM (*Continued*)

	Mechanism						*A* (cm/mol/s)	Exp of T	*E* (kJ/mol)
122	CH_3	$+CO$		$\rightarrow CH_2CO$	$+H$		1.08E + 12	0.00	157.01
123	CH_2CO	$+O$		$\rightarrow CHO$	$+CHO$		1.80E + 12	0.00	5.60
124	CHO	$+CHO$		$\rightarrow CH_2CO$	$+O$		4.48E + 10	0.00	127.36
125	CH_2CO	$+OH$		$\rightarrow CH_2O$	$+CHO$		1.00E + 13	0.00	0.00
126	CH_2O	$+CHO$		$\rightarrow CH_2CO$	$+OH$		7.14E + 12	0.00	68.46
127	CH_2CO	$+M^*$		$\rightarrow CH_2$	$+CO$	$+M^*$	1.00E + 16	0.00	248.00
128	CH_2	$+CO$	$+M^*$	$\rightarrow CH_2CO$	$+M^*$		7.72E + 13	0.00	−62.88
129	C_2H_3	$+H$		$\rightarrow H_2$	$+C_2H_2$		2.00E + 13	0.00	0.00
130	H_2	$+C_2H_2$		$\rightarrow C_2H_3$	$+H$		4.21E + 13	0.00	247.59
131	C_2H_3	$+O$		$\rightarrow CH_2CO$	$+H$		3.00E + 13	0.00	0.00
132	CH_2CO	$+H$		$\rightarrow C_2H_3$	$+O$		3.92E + 14	0.00	333.88
133	C_2H_3	$+O_2$		$\rightarrow CH_2O$	$+CHO$		1.50E + 12	0.00	0.00
134	C_2H_3			$\rightarrow C_2H_2$	$+H$		1.60E + 32	−5.50	193.50
135	C_2H_2	$+H$		$\rightarrow C_2H_3$			8.35E + 31	−5.50	4.27
136	CH_3CO	$+H$		$\rightarrow CH_2CO$	$+H_2$		2.00E + 13	0.00	0.00
137	CH_2CO	$+H_2$		$\rightarrow CH_3CO$	$+H$		4.13E + 13	0.00	247.21
138	CH_3CO	$+O$		$\rightarrow CH_3$	$+CO_2$		2.00E + 13	0.00	0.00
139	CH_3	$+CO_2$		$\rightarrow CH_3CO$	$+O$		3.16E + 14	0.00	476.45
140	CH_3CO	$+CH_3$		$\rightarrow C_2H_6$	$+CO$		5.00E + 13	0.00	0.00
141	C_2H_6	$+CO$		$\rightarrow CH_3CO$	$+CH_3$		5.43E + 15	0.00	320.22
142	CH_3CO			$\rightarrow CH_3$	$+CO$		2.30E + 26	−5.00	75.20
143	CH_3	$+CO$		$\rightarrow CH_3CO$			1.82E + 25	−5.00	30.00
144	C_2H_4	$+H$		$\rightarrow C_2H_3$	$+H_2$		1.50E + 14	0.00	42.70
145	C_2H_3	$+H_2$		$\rightarrow C_2H_4$	$+H$		9.22E + 12	0.00	58.45
146	C_2H_4	$+O$		$\rightarrow CH_3CO$	$+H$		1.60E + 09	1.20	3.10
147	C_2H_4	$+OH$		$\rightarrow C_2H_3$	$+H_2O$		3.00E + 13	0.00	12.60
148	C_2H_3	$+H_2O$		$\rightarrow C_2H_4$	$+OH$		7.95E + 12	0.00	91.01
149	C_2H_4	$+CH_3$		$\rightarrow C_2H_3$	$+CH_4$		4.20E + 11	0.00	46.50
150	C_2H_3	$+CH_4$		$\rightarrow C_2H_4$	$+CH_3$		6.81E + 11	0.00	65.57
151	C_2H_4	$+M^*$		$\rightarrow C_2H_2$	$+H_2$	$+M^*$	2.50E + 17	0.00	319.80
152	C_2H_2	$+H_2$		$\rightarrow C_2H_4$	$+M^*$		8.01E + 15	0.00	146.33
153	CH_3CHO	$+H$		$\rightarrow CH_3CO$	$+H_2$		4.00E + 13	0.00	17.60
154	CH_3CO	$+H_2$		$\rightarrow CH_3CHO$	$+H$		7.57E + 12	0.00	98.28
155	CH_3CHO	$+O$		$\rightarrow CH_3CO$	$+OH$		5.00E + 12	0.00	7.50
156	CH_3CO	$+OH$		$\rightarrow CH_3CHO$	$+O$		4.15E + 11	0.00	80.17
157	CH_3CHO	$+OH$		$\rightarrow CH_3CO$	$+H_2O$		8.00E + 12	0.00	0.00
158	CH_3CO	$+H_2O$		$\rightarrow CH_3CHO$	$+OH$		6.53E + 12	0.00	143.34
159	CH_3CHO	$+HO_2$		$\rightarrow CH_3CO$	$+H_2O_2$		1.70E + 12	0.00	44.80
160	CH_3CO	$+H_2O_2$		$\rightarrow CH_3CHO$	$+HO_2$		4.16E + 11	0.00	57.59
161	CH_3CHO	$+CH_2$		$\rightarrow CH_3CO$	$+CH_3$		2.50E + 12	0.00	15.90
162	CH_3CO	$+CH_3$		$\rightarrow CH_3CHO$	$+CH_2$		2.34E + 12	0.00	115.06
163	CH_3CHO	$+CH_3$		$\rightarrow CH_3CO$	$+CH_4$		8.50E + 10	0.00	25.10
164	CH_3CO	$+CH_4$		$\rightarrow CH_3CHO$	$+CH_3$		4.25E + 11	0.00	109.10
165	CH_3CHO			$\rightarrow CH_3$	$+CHO$		2.00E + 15	0.00	331.00
166	CH_3	$+CHO$		$\rightarrow CH_3CHO$			4.60E + 12	0.00	−10.01
167	C_2H_5	$+H$		$\rightarrow CH_3$	$+CH_3$		3.00E + 13	0.00	0.00
168	CH_3	$+CH_3$		$\rightarrow C_2H_5$	$+H$		3.66E + 12	0.00	37.36
169	C_2H_5	$+O$		$\rightarrow CH_3CHO$	$+H$		5.00E + 13	0.00	0.00
170	CH_3CHO	$+H$		$\rightarrow C_2H_5$	$+O$		6.88E + 14	0.00	295.40
171	C_2H_5	$+O_2$		$\rightarrow HO_2$	$+C_2H_4$		2.00E + 12	0.00	20.90
172	HO_2	$+C_2H_4$		$\rightarrow C_2H_5$	$+O_2$		4.61E + 12	0.00	53.12
173	C_2H_5	$+CH_3$		$\rightarrow C_3H_8$			7.00E + 12	0.00	0.00
174	C_3H_8			$\rightarrow C_2H_5$	$+CH_3$		1.19E + 16	0.00	337.08
175	C_2H_5	$+C_2H_5$		$\rightarrow C_2H_4$	$+C_2H_6$		1.40E + 12	0.00	0.00
176	C_2H_4	$+C_2H_6$		$\rightarrow C_2H_5$	$+C_2H_5$		3.89E + 14	0.00	239.61
177	C_2H_5			$\rightarrow C_2H_4$	$+H$		1.00E + 43	−9.10	224.10
178	C_2H_4	$+H$		$\rightarrow C_2H_5$			1.66E + 43	−9.10	60.94

CHEMICAL REACTION MECHANISM (*Continued*)

	Mechanism				*A* (cm/mol/s)	Exp of T	*E* (kJ/mol)
179	C_2H_6	$+H$	$\rightarrow H_2$	$+C_2H_5$	5.40E + 02	3.50	21.80
180	H_2	$+C_2H_5$	$\rightarrow C_2H_6$	$+H$	1.30E + 01	3.50	55.84
181	C_2H_6	$+O$	$\rightarrow OH$	$+C_2H_5$	3.00E + 07	2.00	21.40
182	OH	$+C_2H_5$	$\rightarrow C_2H_6$	$+O$	3.17E + 05	2.00	47.43
183	C_2H_6	$+OH$	$\rightarrow H_2O$	$+C_2H_5$	6.30E + 06	2.00	2.70
184	H_2O	$+C_2H_5$	$\rightarrow C_2H_6$	$+OH$	6.55E + 05	2.00	99.40
185	C_2H_6	$+HO_2$	$\rightarrow H_2O_2$	$+C_2H_5$	6.00E + 12	0.00	81.20
186	H_2O_2	$+C_2H_5$	$\rightarrow C_2H_6$	$+HO_2$	1.87E + 11	0.00	47.35
187	C_2H_6	$+CH_3$	$\rightarrow C_2H_5$	$+CH_4$	5.50E − 01	4.00	34.70
188	C_2H_5	$+CH_4$	$\rightarrow C_2H_6$	$+CH_3$	3.50E − 01	4.00	72.06
189	C_2H_6	$+CH_2$	$\rightarrow CH_3$	$+C_2H_5$	2.20E + 13	0.00	36.30
190	CH_3	$+C_2H_5$	$\rightarrow C_2H_6$	$+CH_2$	2.63E + 12	0.00	88.82
191	C_2H_6	$+CH$	$\rightarrow H$	$+C_3H_6$	1.10E + 14	0.00	−1.10
192	H	$+C_3H_6$	$\rightarrow C_2H_6$	$+CH$	2.38E + 15	0.00	260.21
		5. C-3 Mechanism					
193	C_3H_8	$+H$	$\rightarrow N\text{-}C_3H_7$	$+H_2$	1.30E + 14	0.00	40.60
194	$N\text{-}C_3H_7$	$+H_2$	$\rightarrow C_3H_8$	$+H$	2.61E + 12	0.00	58.28
195	C_3H_8	$+H$	$\rightarrow I\text{-}C_3H_7$	$+H_2$	1.00E + 14	0.00	34.90
196	$I\text{-}C_3H_7$	$+H_2$	$\rightarrow C_3H_8$	$+H$	5.13E + 12	0.00	64.51
197	C_3H_8	$+O$	$\rightarrow N\text{-}C_3H_7$	$+OH$	3.00E + 13	0.00	24.10
198	$N\text{-}C_3H_7$	$+OH$	$\rightarrow C_3H_8$	$+O$	2.65E + 11	0.00	33.77
199	C_3H_8	$+O$	$\rightarrow I\text{-}C_3H_7$	$+OH$	2.60E + 13	0.00	18.70
200	$I\text{-}C_3H_7$	$+OH$	$\rightarrow C_3H_8$	$+O$	5.86E + 11	0.00	40.30
201	C_3H_8	$+OH$	$\rightarrow N\text{-}C_3H_7$	$+H_2O$	6.30E + 06	2.00	2.70
202	$N\text{-}C_3H_7$	$+H_2O$	$\rightarrow C_3H_8$	$+OH$	5.46E + 05	2.00	83.05
203	C_3H_8	$+OH$	$\rightarrow I\text{-}C_3H_7$	$+H_2O$	1.20E + 08	1.46	−0.80
204	$I\text{-}C_3H_7$	$+H_2O$	$\rightarrow C_3H_8$	$+OH$	2.66E + 07	1.46	91.48
205	C_3H_8	$+HO_2$	$\rightarrow N\text{-}C_3H_7$	$+H_2O_2$	6.00E + 12	0.00	81.20
206	$N\text{-}C_3H_7$	$+H_2O_2$	$\rightarrow C_3H_8$	$+HO_2$	1.56E + 11	0.00	31.00
207	C_3H_8	$+HO_2$	$\rightarrow I\text{-}C_3H_7$	$+H_2O_2$	2.00E + 12	0.00	71.10
208	$I\text{-}C_3H_7$	$+H_2O_2$	$\rightarrow C_3H_8$	$+HO_2$	1.33E + 11	0.00	32.83
209	C_3H_8	$+CH_3$	$\rightarrow N\text{-}C_3H_7$	$+CH_4$	7.50E + 12	0.00	62.50
210	$N\text{-}C_3H_7$	$+CH_4$	$\rightarrow C_3H_8$	$+CH_3$	3.98E + 12	0.00	83.50
211	C_3H_8	$+CH_3$	$\rightarrow I\text{-}C_3H_7$	$+CH_4$	4.30E + 12	0.00	55.50
212	$I\text{-}C_3H_7$	$+CH_4$	$\rightarrow C_3H_8$	$+CH_3$	5.83E + 12	0.00	88.43
213	$N\text{-}C_3H_7$	$+H$	$\rightarrow C_3H_8$		2.00E + 13	0.00	0.00
214	C_3H_8		$\rightarrow N\text{-}C_3H_7$	$+H$	4.01E + 15	0.00	419.13
215	$I\text{-}C_3H_7$	$+H$	$\rightarrow C_3H_8$		2.00E + 13	0.00	0.00
216	C_3H_8		$\rightarrow I\text{-}C_3H_7$	$+H$	1.57E + 15	0.00	407.20
217	$N\text{-}C_3H_7$	$+O_2$	$\rightarrow C_3H_6$	$+HO_2$	1.00E + 12	0.00	20.90
218	C_3H_6	$+HO_2$	$\rightarrow N\text{-}C_3H_7$	$+O_2$	5.11E + 12	0.00	82.88
219	$I\text{-}C_3H_7$	$+O_2$	$\rightarrow C_3H_6$	$+HO_2$	1.00E + 12	0.00	12.50
220	C_3H_6	$+HO_2$	$\rightarrow I\text{-}C_3H_7$	$+O_2$	2.00E + 12	0.00	62.55
221	$I\text{-}C_3H_7$		$\rightarrow C_3H_6$	$+H$	2.00E + 14	0.00	161.90
222	C_3H_6	$+H$	$\rightarrow I\text{-}C_3H_7$		2.89E + 14	0.00	16.56
223	$N\text{-}C_3H_7$		$\rightarrow C_2H_4$	$+CH_3$	3.00E + 14	0.00	139.00
224	C_2H_4	$+CH_3$	$\rightarrow N\text{-}C_3H_7$		5.88E + 13	0.00	57.89
225	$N\text{-}C_3H_7$		$\rightarrow C_3H_6$	$+H$	1.00E + 14	0.00	156.10
226	C_3H_6	$+H$	$\rightarrow N\text{-}C_3H_7$		3.69E + 14	0.00	22.69
227	C_3H_6	$+O$	$\rightarrow CH_3CO$	$+CH_3$	5.00E + 12	0.00	1.90
228	C_3H_6	$+OH$	$\rightarrow CH_3CHO$	$+CH_3$	2.00E + 13	0.00	12.80

Third-Body Effectivities

$M^* = 1.00\ H_2 + 6.50\ H_2O + 0.40\ O_2 + 0.40\ N_2 + 0.75\ CO + 1.50\ CO_2 + 3.00\ CH_4 / C_3H_8$

M has equal effectivity for all species

REFERENCES

1. Bray, K. N. C., Libby, P. A., and Moss, J. B., *Combust. Sci. Technol.* 41:143 (1984).
2. Peters, N., *Twenty-First Symposium (International) on Combustion*, The Combustion Institute, Pittsburgh, 1986, p. 1231.
3. Cant, R. S., and Bray, K. N. C., *Twenty-Second Symposium (International) on Combustion*, The Combustion Institute, Pittsburgh, 1988.
4. Dixon-Lewis, G., Presented at the Workshop of Gas Flame Structure, Novosibirsk, 1986.
5. Dixon-Lewis, G., *Prog. Astronaut. Aeronaut.* 113:166 (1988).
6. Giovangigli, V., and Smooke, M. D., *J. Comp. Phys.* 68:327 (1987).
7. Giovangigli, V., and Smooke, M. D., *Combust. Sci. Technol.* 53:23 (1987).
8. Stahl, G., Warnatz, J., and Rogg, B., *Prog. Astronaut. Aeronaut.* 113:195 (1988).
9. Rogg, B., *Combust. Flame* 73:45 (1988).
10. Kee, R. J., Miller, J. A., Evans, G. H., and Dixon-Lewis, G., *Twenty-Second Symposium (International) on Combustion*, The Combustion Institute, Pittsburgh, 1988.
11. Ishizuka, S., and Law, C. K., *Nineteenth Symposium (International) on Combustion*, The Combustion Institute, Pittsburgh, 1982, p. 327.
12. Tsuji, H. and Yamaoka, I., *Nineteenth Symposium (International) on Combustion*, The Combustion Institute, Pittsburgh, 1982, p. 1533.
13. Sato, J., *Nineteenth Symposium (International) on Combustion*, The Combustion Institute, Pittsburgh, 1982, p. 1541.
14. Sohrab, S. H., Ye, Z. Y., and Law C. K., *Twentieth Symposium (International) on Combustion*, The Combustion Institute, Pittsburgh, 1984, p. 1957.
15. Mendes-Lopes, J. M. C., and Daneshyar, H., *Combust. Flame* 60:29 (1985).
16. Law, C. K., Zhu, D. L., and Yu, G., *Twenty-First Symposium (International) on Combustion*, The Combustion Institute, Pittsburgh, 1986.
17. Haworth, D. C., Drake, M. C., Pope, S. B., and Blint, R. J., *Twenty-Second Symposium (International) on Combustion*, The Combustion Institute, Pittsburgh, 1988.
18. Saitoh, T., and Otsuka, Y., *Combust. Sci. Technol.* 12:135 (1976).
19. Sivashinsky, G. I., *Acta Astronaut.* 3:889 (1976).
20. Buckmaster, J., *Seventeenth Symposium (International) on Combustion*, The Combustion Institute, Pittsburgh, 1978, p. 835.
21. Libby, P. A., and Williams, F. A., *Combust. Sci. Technol.* 37:221 (1984).
22. Williams, F. A., *Combustion Theory*, 2nd ed., Benjamin/Cummings, Menlo Park, CA, 1985.
23. Warnatz, J., in *Combustion Chemistry*, (W. C. Gardiner, Ed.), Springer, New York (1984).
24. Warnatz, J., *Eighteenth Symposium (International) on Combustion*, The Combustion Institute, Pittsburgh, 1981, p. 369.
25. Frenklach, M., and Warnatz, J., *Combust. Sci. Technol.* 51:265 (1987).
26. Warnatz, J., SANDIA Report 83-8855, Sandia National Laboratories, Livermore, CA, 1983.
27. *JANAF Thermochemical Tables*, 2nd ed., National Bureau of Standards, Washington, D.C., 1971.
28. Mason, E. A., and Monchick, L., *J. Chem. Phys.* 36:1622 (1969).
29. Hirschfelder, J. O., Curtiss, C. F., and Bird, R. B., *Molecular Theory of Gases and Liquids*, Wiley, New York, 1964.
30. Maas, U., and Warnatz, J., *Combust. Flame* 74:53 (1988).
31. Deuflhard, P., Hairer, E., and Zugck, J., University of Heidelberg, SFB 123: Technical Report 318, 1985.
32. Deuflhard, P., and Nowak, U., University of Heidelberg, SFB 123: Technical Report 332, 1985.
33. Deuflhard, P., Konrad-Zuse-Zentrum für Informationstechnik Berlin, Technical Report SC-87-3, 1987.
34. Dixon-Lewis, G., Kee, R. J., Rogg, B., Smooke, M. D., Stahl, G., and Warnatz, J., Presented at the 12th ICDERS, University of Michigan, July 23–28, 1989.

Received 25 July 1989; revised 28 April 1990